Academic Journal of Applied Mathematical Sciences
ISSN(e): 2415-2188, ISSN(p): 2415-5225
Vol. 4, Issue. 4, pp: 22-33, 2018
URL: http://arpgweb.com/?ic=journal&journal=17&info=aims

Academic Research Publishing Group

Original Research Open Access

Heat Transfer through Parallel Plate Microchannels at Symmetric and Asymmetric Constant Wall Temperature

Md. Tajul Islam
Department of Mathematics, Begum Rokeya University, Rangpur, Bangladesh

Abstract

Forced convective heat transfer in parallel microchannels with asymmetric and symmetric wall thermal conditions under hydrodynamically and thermally fully developed flow is investigated using control volume technique for steady, two dimensional flow. Incompressible Navier-Stokes and energy equations are solved applying velocity slip and temperature jump boundary conditions on the walls. Simulations are validated comparing with the experimental results available in the literature. Simulations are performed for different temperature difference between the walls and the gas as well as the inlet velocity and ambient pressure conditions. Either the wall heating or wall cooling cases are examined taking Nitrogen gas as the working fluid. The influences of Knudsen number, Reynolds number and temperature difference on Nusselt number are observed. It is shown here that for asymmetric wall thermal condition for temperature dependent thermal conductivity the Nusselt number is lower for higher temperature difference where as for symmetric wall thermal condition Nusselt number is higher for higher temperature difference.

Keywords: Nusselt number; Wall heating; Wall cooling; Knudsen number; Velocity slip; Temperature jump.

1. Introduction

Manufacturing processes of extremely small devices have been developed in recent years. The development of microfabrication enabled the usage of devices having dimensions of microns such as micro heat sink, micro heat exchanger, sensors, actuators, gears, valves etc. Micro-electromechanical systems (MEMS) refer to devices that have a characteristic length of less than 1 mm but more than 1 μm, that combine electrical and mechanical components and that are fabricated using integrated circuit batch processing technologies [1]. The rapid advancements of MEMS (Micro-electromechanical systems) have created the requirements for the dissipation of heat generated by the above devices in an efficient way. Surface effects dominate in small devices. The surface-to-volume ratio for a machine with a characteristic length of 1m is 1 m^{-1}, while that for a MEMS device having a size of 1μm is $10^6 m^{-1}$. The millionfold increase in surface area relative to the mass of the minute device substantially affects the transport of mass, momentum, and energy through the surface [1]. Microchannels have these features of smaller volume and mass with high surface area to volume ratio, and can be used for the removal of maximum heat from small areas. Due to their inherent advantages, microchannel heat sinks have found applications in automotive heat exchangers, cooling of high power electronic devices, aerospace industry, etc. Fundamental understanding of fluid flow and heat transfer in microchannels is essential in designing of microfluidic devices.

Microscale fluid flow and heat transfer differs from that of the macroscale. At macroscale the classical conservation equations are applied with the usual noslip for the velocity boundary condition and no-temperature jump for the thermal boundary condition. These two boundary conditions are valid only if the fluid flow adjacent to surface is in thermodynamic equilibrium. At microscale the fluid particle on the surface no longer reaches the velocity or temperature of the surface and the velocity slip and temperature jump must be applied to the surface. The velocity slip and temperature jump are the consequence of rarefaction. The Knudsen number is the measure of degree of rarefaction which is the ratio of mean free path to the characteristic length of the problem. λ is the mean free path corresponding to the distance travelled by the molecules between collisions and is defined by

$$\lambda = \frac{k_B T}{\sqrt{2}\pi p \sigma^2} \qquad (1)$$

In parallel plate channel, hydraulic diameter is treated as characteristic length and is defined by $D_h = 2H$ where H is the height of the channel. The appropriate flow and heat transfer models depend on the range of the Knudsen number, defined by $Kn = \lambda / H$. A classification of different flow regimes is given by Schaaf and Chamber [2]. For Kn < 0.001, the fluid can be considered as continuum and the fluid is in local thermodynamic equilibrium. Thus, the Navier-Stokes equations with no-slip and no-temperature jump boundary condition describe the flow behaviors. For the Knudsen number in the range between 0.001 and 0.1, the rarefaction effects become important. This range is referred to as the slip flow regime, where the continuum hypothesis is still valid, but the local thermodynamic equilibrium of the flow near the surface is not maintained. In this range, the Navier-Stokes

*Corresponding Author

equations remain applicable, provided a velocity slip and a temperature jump are taken into account at the surface. For the Knudsen number in the range 0.1< *Kn* <10, the flow is referred to as the transitional regime where the continuum approach of the Navier–Stokes equations is no longer valid. However, the intermolecular collisions are not yet negligible and should be taken into account. Finally, the range *Kn* > 10 represents the free molecular regime where the intermolecular collisions among the molecules are negligible.

Nomenclature

H : channel height $[\mu m]$
L : length of the channel $[\mu m]$
T : Temperature $[^{\circ}K]$
k_B : Boltzmann constant
p : pressure $[N/m^2]$
Kn : Knudsen number
Kn_o : outlet Knudsen number
R : gas constant $[J/kg.K]$
u, v :velocity components $[m/s]$
q'' : heat flux $[kW]$
Re : Reynolds number
n : normal coordinate on the channel wall
x, y : co-ordinates distances $[\mu m]$
Td : temperature difference $[^{\circ}K]$
c_p : specific heat at constant pressure

Greek symbols

μ :dynamic viscosity $[N.s/m^2]$
ρ :density $[kg/m^3]$
τ :shear stress $[N/m^2]$
σ :molecular diameter, Angstroms
σ_m: tangential momentum accommodation coefficient
σ_T: thermal accommodation coefficient
λ :mean free path $[\mu m]$
α :Thermal diffusivity $[m^2/s]$

Subscripts

i :channel inlet
o :channel outlet
w :wall
g : gas

Tuckerman and Pease [3] first introduced the concept of using microchannels as high performance heat sink in 1981. They fabricated microchannel heat sink in silicon wafer and used water as coolant under laminar flow conditions. They showed that the heat sink dissipated $790W/cm^2$ with the maximum temperature difference between the substrate and the coolant as $71^{\circ}C$.

Peiyi and Little [4] conducted experiments to measure the flow friction and heat transfer characteristics of gaseous flow in microchannels and found that the convective heat transfer characteristics departed from the typical experimental results for conventional sized channels. They reported that the flow transition from laminar to turbulent occurs at relatively low Reynolds number resulted in improved heat transfer. Peng and Peterson [5] conducted experimental investigation in microchannels of varying sizes. Their experiments showed a decrease of Nusselt number in the laminar flow regime but increase of Nusselt number in the turbulent flow regime with the increasing Reynolds number. They also showed that a small inlet temperature and a large velocity result in higher heat transfer coefficients.

Peng, *et al.* [6] performed experiments on rectangular microchannels of different dimensions and found the Nusselt number to lie below the predicted values of Dittus-Boelter equation. Nicolas, *et al.* [7] investigated constant wall temperature convective heat transfer of gaseous flow in two-dimensional micro and nano-channels. They concluded that convective transfer in low speed flows in the slip flow regime can be captured by slip-corrected continuum flows that neglect viscous dissipation, expansion cooling and thermal creep. Wu and Cheng [8] performed experimental investigation on laminar convective heat transfer and pressure drop in trapezoidal silicon microchannels. They found that the Nusselt number and friction constant increase with the increase of surface roughness and this increase is more pronounced at larger Reynolds numbers.

Owhaib and Palm [9] conducted experimental investigation of heat through microchannels with circular geometry having inner diameter of 1.7, 1.2 and 0.8 *mm*. The results were compared to microscale and macroscale correlations from the literature. The comparison shows that the classical correlations were in good agreement with the experimental data but none of the microscale correlations were in agreement with the experimentally obtained data.

Chien-Hsin [10] studied forced convection flow in a microchannel with constant wall temperature including viscous dissipation. The result reveals that the fully developed Nusselt number is found to decrease with increasing parameter β. When the viscous dissipation effect is accounted for, the local Nusselt number exhibits a jump at certain axial position and then reaches its final value. Furthermore, including viscous dissipation produces a noticeable increase in the fully developed Nusselt number.

In light of the above discussion it makes sense that the heat transfer in microchannels has been studied by a number of investigators, and has been compared and contrasted with the behavior at conventional (i.e., larger-sized) length scales. However, there have been wide discrepancies among different sets of published results. Some authors reported higher heat transfer whereas the others reported lower heat transfer through microchannels compared to the

conventional channels. In order to design and fabricate micro-devices properly, insight characteristics of fluid flow and heat transfer in microchannels must be understood. So it is obvious that more investigations are required which is the driving force to conduct the present investigation.

The objective of the present study is to investigate the heat transfer characteristics in parallel plate channels under velocity slip or temperature jump or both boundary conditions. Either the wall heating or wall cooling cases are examined on symmetric or asymmetric wall thermal conditions. The influences of Reynolds and Knudsen numbers on Nusselt numbers are investigated. The free stream temperature and the temperature of the walls are set to constant. The temperature difference between the wall and the fluid plays an important role on heat transfer and consequently the effect of temperature difference on velocity slip, temperature jump and Nusselt number are investigated.

2. Model Development

2.1. Problem description

Nitrogen gas flow through a two dimensional channel of length L with walls those are apart at a distance H are considered. The following Figure 1, shows the geometry and coordinate system of the channel.

Figure-1. Schematic diagram of the channel

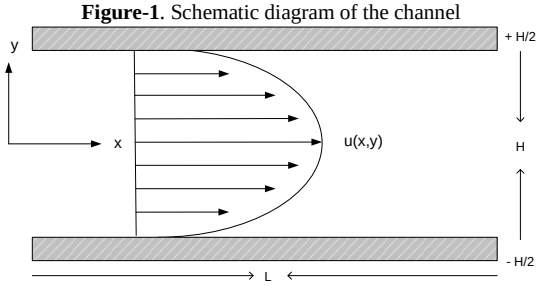

The flow domain is bounded by $0 \le x \le L$ and $-\frac{H}{2} \le y \le \frac{H}{2}$ where *L* is sufficiently large for the flow to be fully developed for both hydrodynamically and thermally. Constant wall temperature for both wall heating and wall cooling are considered. Usual continuum approach is coupled with the two microscale phenomena; the velocity slip and the temperature jump boundary conditions. A series of simulations are performed imposing various sets of combinations of the above phenomena on the walls. Required Reynolds numbers, Knudsen numbers and Nusselt numbers are obtained by changing the inlet velocity, wall temperature and pressure.

Nusselt number is defined as

$$Nu = \frac{2Hq''}{k(T_w - T_b)}$$

where k is the fluid thermal conductivity and is a function of temperature.

Reynolds number is defined as

$$\mathrm{Re} = \frac{\rho u_m D_h}{\mu}$$

Where u_m is the mean velocity at the location of interest of the channel. Mean velocity is calculated by the following expression as it is defined in Patric and William [11].

$$u_m = \frac{H^2}{12\mu}\frac{dp}{dx}\left[1 + 6\left(\frac{\lambda}{H}\right)\left(\frac{2-\sigma_m}{\sigma_m}\right)\right]$$

and Bulk temperature is defined by

$$T_b = \frac{\int \rho u T dA}{\int \rho u dA}$$

where *A* is the cross sectional area of the channel and *u* is the streamwise velocity component.

2.2. Governing Equations

Nitrogen gas flow and heat transfer between *2D* parallel plate channel is assumed to be steady and laminar. The Three basic laws of conservation of mass, momentum and energy are solved for incompressible flow of Newtonian fluid. The governing equations can be expressed in Cartesian coordinates as:

The continuity equation:

$$\frac{\partial u}{\partial x}+\frac{\partial v}{\partial y}=0 \tag{2}$$

The Navier-Stokes equations:

$$\rho\left(u\frac{\partial u}{\partial x}+v\frac{\partial u}{\partial y}\right)=-\frac{\partial p}{\partial x}+\mu\left(\frac{\partial^2 u}{\partial x^2}+\frac{\partial^2 u}{\partial y^2}\right) \tag{3}$$

$$\rho\left(u\frac{\partial v}{\partial x}+v\frac{\partial v}{\partial y}\right)=-\frac{\partial p}{\partial y}+\mu\left(\frac{\partial^2 v}{\partial x^2}+\frac{\partial^2 v}{\partial y^2}\right) \tag{4}$$

The energy equation:

$$\left(u\frac{\partial T}{\partial x}+v\frac{\partial T}{\partial y}\right)=\frac{1}{\rho c_p}\frac{\partial}{\partial y}\left(k\frac{\partial T}{\partial y}\right)+\frac{\nu}{c_p}\left(\frac{\partial u}{\partial y}\right)^2 \tag{5}$$

2.3. Boundary Conditions

The slip velocity condition was proposed by Maxwell [12] and the temperature jump boundary condition by Smoluchowski [13]. To impose the velocity slip and temperature jump boundary conditions on the walls, UDF routine (User defined functions) are developed and associated with the Fluent solver. The proposed velocity slip boundary conditions are expressed as

$$u_{slip}=u_{fluid}-u_{wall}=\frac{2-\sigma_m}{\sigma_m}\lambda\left(\frac{\partial u}{\partial x}+\frac{\partial u}{\partial y}\right)_{wall}+\frac{3}{4}\frac{\mu}{\rho T_{fluid}}\left(\frac{\partial T}{\partial x}\right)_{wall} \tag{6}$$

And the temperature jump boundary conditions are expressed as

$$T_{fluid}-T_{wall}=\left(\frac{2-\sigma_T}{\sigma_T}\right)\frac{2\gamma}{\gamma+1}\frac{\lambda}{Pr}\left(\frac{\partial T}{\partial y}\right)_{wall} \tag{7}$$

where $Pr=\frac{\mu c_p}{k}$ is the Prandtl number.

The tangential-momentum-accommodation coefficient σ_m =1 and the thermal-accommodation coefficient σ_T =1 describe the gas-wall interactions.

It is stated earlier that the constant wall temperature boundary conditions are implied on the walls. Simulations are performed either in wall heating (hot wall) or in wall cooling (cold wall) conditions. To impose constant wall temperature boundary condition, two cases are considered separately:

Case 1: Investigations are operated on asymmetric wall thermal conditions where viscous dissipation is not considered. The inlet and the outlet boundaries are velocity inlet and the pressure outlet respectively. The uniform inlet temperature T_{in} at *x = 0* and the lower wall constant temperature T_{lw} at $y=-H/2$ are kept equal $T_{in}=T_{lw}$, which is lower than the upper wall temperature T_{uw} at $y=H/2$ and the difference between the upper and lower wall temperature varies from 100°*K* to 600°*K*.

Case 2: Simulations are performed under symmetric wall thermal conditions incorporating viscous dissipation. The inlet and the outlet boundaries are velocity inlet and the pressure outlet respectively. The constant temperature of both the lower and the upper walls are the same $T_{uw}=T_{lw}$ and is higher than the uniform inlet temperature T_{in} at *x = 0* and the difference between T_{in} and T_{uw} or T_{lw} varies from 20°*K* to 500°*K*. To find the effect of temperature

difference on Nusselt numbers, the temperature differences are changed as needed for different simulations, keeping all the flow conditions the same.

2.4. Numerical Method

2.4.1. Discretization

In the present study, the governing equations are discretized using a control volume based technique. The governing equations are first integrated about each control volume to ensure that the conservation equations are automatically satisfied within each control volume. The net flux through the control volume boundary is the sum of integrals over the control volume faces. Discretization of the governing equation for transport of a scalar quantity ϕ can be written in integral form for an arbitrary control volume V according to Ansys Inc [14] as:

$$\oint \rho \phi \vec{V}.d\vec{A} = \oint \Gamma_{\phi} \nabla \phi.d\vec{A} + \int S_{\phi} dV \tag{8}$$

Where, $\vec{A}$ is the area surface vector, Γ_{ϕ} is the diffusion coefficient for ϕ and S_{ϕ} is the source of ϕ per unit volume. Eq. (8) is applied to each control volume of cell in the computational domain. Discretization of Eq. (8) on a given cell yields

$$\sum_{f}^{N_{faces}} \rho_f \vec{V}_f \phi_f .\vec{A} = \sum_{f}^{N_{faces}} \Gamma_{\phi} (\nabla \phi)_f .\vec{A}_f + S_{\phi} V \tag{9}$$

Where, N_{faces} is the number of faces enclosing a cell, ϕ_f is the value of ϕ convected through face f and $\rho_f \vec{V}.\vec{A}_f$ is the mass flux through face *f*.

The discretized scalar transport eq. (9) contains the unknown scalar variable ϕ at the cell center as well as the unknown values in surrounding neighbor cells. This equation will, in general, be non-linear with respect to these variables. A linearized form of Eq. (9) can be written as

$$a_P \phi_P = \sum_{nb} a_{nb} \phi_{nb} + b$$

Here the subscript *nb* refers to the neighboring cells of *P*. The coefficients a_P and a_{nb} are the linearized coefficients of ϕ_P and ϕ_{nb} and will be different for every cell in the domain at every iteration.

By default, all variable values are calculated and stored at the cell centers. However the face values ϕ_f are required for the convection terms in Eq. (9) and must be interpolated from the cell center values. A second order upwind scheme is used to predict the value of ϕ at the faces.

2.4.2. Pressure Velocity Coupling

Density is constant for incompressible flow and hence not linked to the pressure. In this case coupling between pressure and velocity introduces a constraint in the solution of the flow field. The associated problems are resolved by adopting an iterative solution strategy SIMPLE (Semi-Implicit Method for Pressure-Linked Equations) algorithm.

To initiate the SIMPLE calculation process a pressure field p^* is guessed. Discretized *x-momentum* and *y-momentum* equations are solved using the guessed pressure field to yield velocity components u^* and v^*. Now the correction p' is defined as the difference between correct pressure field *p* and the guessed pressure field p^*, so that

$$p = p^* + p'$$

Similarly we define velocity corrections u' and v' to relate the guessed velocities u^* and v^* to the correct velocities *u* and *v* respectively so that:

$$u = u^* + u'$$
$$v = v^* + v'$$

Substitution of the correct pressure field *p* into the momentum equations yields the correct velocity field (*u*, *v*). Discretized *x-momentum* and *y-momentum* equations link the correct velocity fields with the correct pressure field.

The computations are considered to be converged when the residues for continuity, momentum and energy are less than 10^{-6}.

2.5. Grid dependency Test

To evaluate the grid size effect, grid dependency tests are carried out. Keeping all the conditions unchanged, average Nusselt number for three different sizes of grid 31×1201, 41×1501 and 51×1801 at fixed Knudsen number 0.05 and Reynolds number 1.0 are investigated for an incompressible flow applying velocity slip and temperature jump boundary conditions and the results are listed in Table 1. The table shows that the relative difference of average Nusselt number for grid sizes 31×1201 and 41×1501 is 0.33% and for grid sizes 41×1501 and 51×1801 is 0.13% respectively. In both the cases the relative difference of Nusselt number is small and negligible. For convenience, we used grid size 41×1501.

Table-1. Grid dependence test of the average velocity under three sizes of grids

Grid size	Average velocity
31×1201	3.60845
41×1501	3.62042
51×1801	3.62513

2.6. Validation

The result of the present study is compared and validated with the results published in the literature. Fig. 2 shows the comparison of the distribution of Nusselt numbers from the analytical results by Orhan and Mete [15], and from the present study with the same conditions. The Prandtl number and the Brinkman number were fixed to 0.7 and 0.01 respectively. The square symbols represent the analytical results and the solid line represents the results from present work and the agreement is satisfactory.

Figure-2. Comparison of Nusselt number distribution for different Knudsen numbers (Pr = 0.7, Br = 0.01)

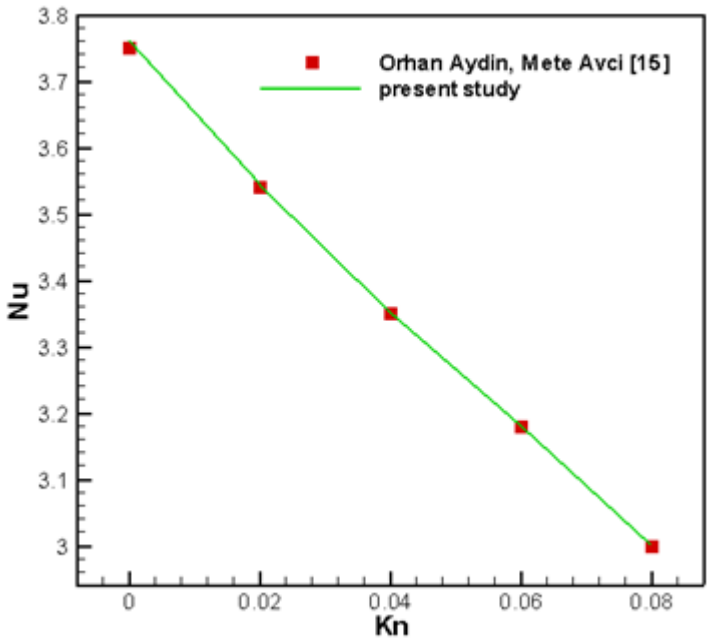

2.7. Results and Discussion

In this study, we investigated the effect of temperature difference as well as Reynolds and Knudsen numbers on Nusselt numbers. The difference between the free stream temperature and the wall temperature is termed as temperature difference (T_d). In our simulation the maximum Mach number is 0.037 and the maximum density variations in the inlet and the outlet positions are 9.17%. So the flow can be safely considered as incompressible flow. Mainly two types of thermal conditions namely, asymmetric and symmetric wall conditions are used on the walls.

Case 1: In case of asymmetric wall thermal condition, the free stream temperature and the bottom wall temperature are kept equal to $200^{\circ}K$ and the temperature difference between the top and bottom walls vary from $100^{\circ}K$ to $600^{\circ}K$. Fluid properties are considered constant except thermal conductivity which is a function of temperature and the viscous dissipation is not included here. Under the conditions of Case 1, the results obtained through our investigations are discussed and displayed by Figure 3 and Figure 4.

Figure 3 shows the Nusselt numbers distribution for different temperature differences between the wall and the fluid as stated in Case 1 where the Reynolds number and Knudsen numbers are kept fixed at 1.0 and 0.025 respectively. In this case fluid bulk temperature is lower than the top wall temperature. Since thermal conductivity increases with the increase of wall temperature, as a result the Nusselt numbers are lower for higher temperature difference. From the figure we see that as the temperature difference increases, the Nusselt number decreases. It is

obvious from the Figure 2 and Figure 3 that the Nusselt number decreases for the increase of both Knudsen number and temperature difference.

The simultaneous effect of Reynolds number, Knudsen number and temperature difference on Nusselt numbers are expressed through the Figure 4. The free stream temperature and the bottom wall temperature are kept at $200^{\circ}K$ and the temperature difference between the top and bottom walls vary from $100^{\circ}K$ to $600^{\circ}K$. Reynolds numbers and Knudsen numbers vary from 1.0 to 4.0 and 0.002 to 0.07 respectively. It is evident from the figure that for lower Knudsen number, the effect of Reynolds number on Nusselt number is negligible but for comparatively higher Knudsen number the Nusselt number increases with the increase of Reynolds number.

Figure-3. Nusselt number distribution for fixed Knudsen number

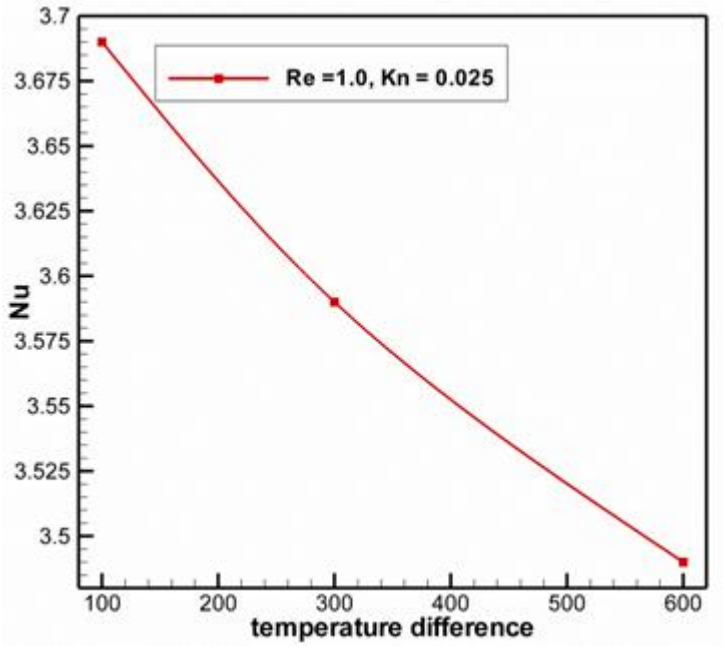

The figure shows the lowest Nusselt numbers distribution for the combined effect of Reynolds number 1.0 and temperature difference $600^{\circ}K$. Keeping Reynolds number fixed to 1.0, if temperature difference is decreased from $600^{\circ}K$ to $100^{\circ}K$, the Nusselt number takes higher values.

Figure-4. Effect of Reynolds number and temperature difference on Nusselt number

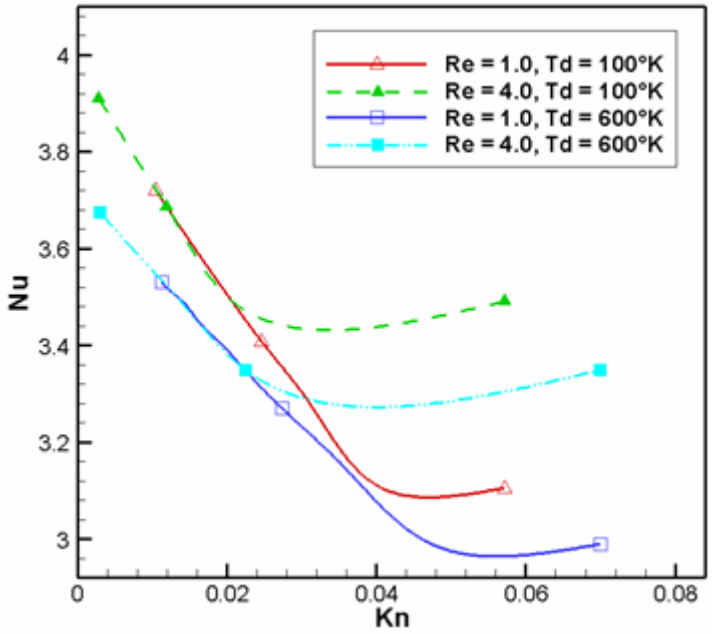

The highest Nusselt numbers distribution is displayed for the combined effect of Reynolds number 4.0 and temperature difference $100^{\circ}K$. Keeping temperature difference fixed to $100^{\circ}K$, if Reynolds number is decreased from 4.0 to 1.0, the Nusselt number takes lower values. It is clear from the above discussion that Reynolds number and temperature difference have opposite effect on Nusselt numbers with the conditions stated in Case1.

Case 2: The investigations are conducted with symmetric wall thermal condition incorporating viscous dissipation. Velocity slip, temperature jump or both the boundary conditions are imposed on the walls as required for our investigation. The temperature difference between the free stream temperature and the wall temperature varies from

$20^{\circ}K$ to $500^{\circ}K$. In case of temperature difference $20^{\circ}K$, the free stream temperature and wall temperature are kept at $300^{\circ}K$ and $320^{\circ}K$ respectively where as in case of temperature difference $500^{\circ}K$, they are kept at $300^{\circ}K$ and $800^{\circ}K$ respectively. Fluid properties are considered as constant.

Figure-5. The effect of temperature difference on velocity slip ($Kn_0 = 0.007$ for $T_d = 20^{\circ}K$ and $Kn_0 = 0.019$ for $T_d = 500^{\circ}K$).

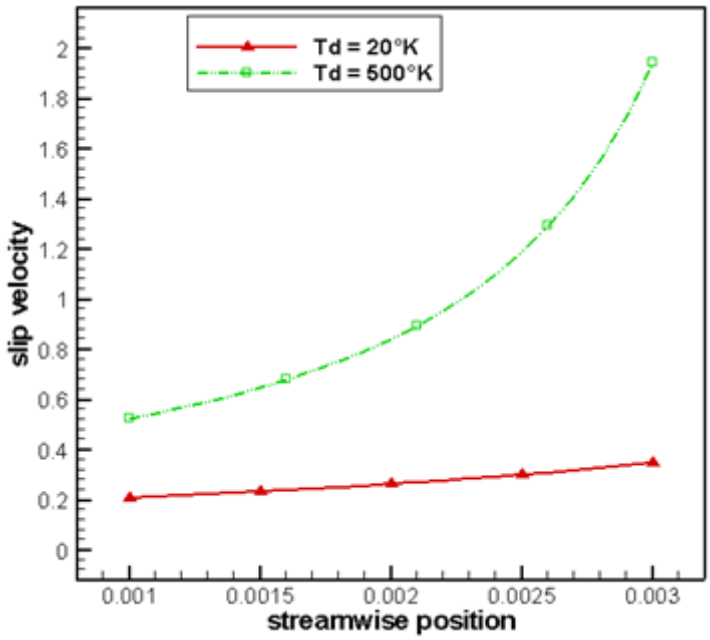

Results obtained by using the thermal conditions described in Case 2 are furnished through Figures 5 - Figure 12.

To find the effect of temperature difference on velocity slip, only the velocity slip boundary condition is applied on the walls. The simulations are performed for two different temperature conditions namely temperature difference $20^{\circ}K$ and $500^{\circ}K$ respectively keeping all other conditions the same and the results are displayed through Figure 5. The dash-dotted line and the solid line show the slip velocity distributions for temperature difference $20^{\circ}K$ and $500^{\circ}K$ respectively. It is evident from the figure that the velocity slip increases with the increase of temperature difference. The increase of velocity slip for higher temperature difference is rapid near the outlet position with compared to velocity slip of lower temperature difference.

The effects of temperature difference on temperature jump are depicted by the Figure 6. To investigate the effect of temperature difference on temperature jump, only the temperature jump boundary condition is imposed on the walls. The temperature difference between the free stream temperature and the wall temperature varies from $20^{\circ}K$ to $500^{\circ}K$. The value of temperature jump is negative and varies to the downward direction. The figure shows that in case of temperature difference $500^{\circ}K$, the magnitude of temperature jump is very large with compare to the case of temperature difference $20^{\circ}K$. Also the decrease of temperature jump near the outlet position is rapid for the temperature difference $500^{\circ}K$.

To investigate the effects of temperature difference on Nusselt numbers, both the velocity slip and temperature jump boundary conditions are imposed on the walls at wall temperature $800^{\circ}K$ and $320^{\circ}K$ resulted temperature difference between the walls and the free stream temperature by $500^{\circ}K$ and $20^{\circ}K$ respectively. The results are displayed through Figure 7.

Figure-6. Comparison of the effect of temperature difference on temperature jump ($Kn_0 = 0.007$ for $T_d = 20^{\circ}K$ and $Kn_0 = 0.019$ for $T_d = 500^{\circ}K$).

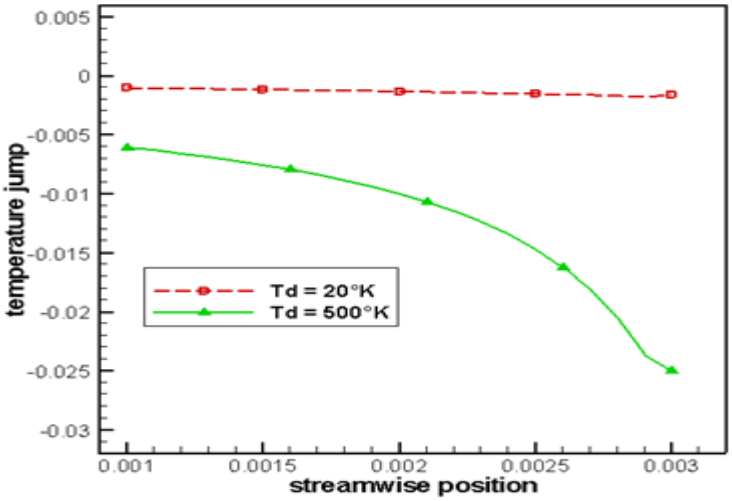

The solid line and the dash-dotted line show the Nusselt number distributions for temperature difference $20^{\circ}K$ and $500^{\circ}K$ and the corresponding outlet Knudsen numbers are 0.007 and 0.019 respectively. The figure shows that the higher the temperature differences between walls and the free stream temperature the higher the Nusselt numbers. In the present case viscous dissipation is considered which contributes to the increase of fluid bulk temperature. The system acts as wall cooling case and the temperature difference between the bulk fluid temperature and the wall temperature is the main driving mechanism of heat transfer. Consequently the Nusselt number increases with the increase of temperature difference.

Nusselt numbers distributions for the boundary conditions; the velocity slip, temperature jump and combined boundary conditions of velocity slip and temperature jump are depicted in Figure 8. In this investigation the temperature difference between the walls and the free stream is $30^{\circ}K$. The solid line shows the Nusselt numbers distribution for both the velocity slip and temperature jump boundary conditions, the dashed line only for velocity slip and the dash-dotted line only for temperature jump boundary conditions. In all the three cases the Knudsen number increases along streamwise direction and the outlet Knudsen number reaches to 0.007. The figure shows that for the case of slip velocity boundary condition the Nusselt number increases along the downstream direction where as in the other two cases the Nusselt numbers decrease. There are small differences between Nusselt numbers for the case of temperature jump and the combined velocity slip and temperature jump boundary conditions. The Nusselt numbers for the case of temperature jump boundary conditions are the lowest.

Hence we can conclude that the velocity slip and temperature jump has opposite effect on Nusselt number. Nusselt number increases by the effect of velocity slip but decreases by the effect of temperature jump. The effect of temperature jump boundary conditions dominates over the effect of velocity slip.

Figure-7. Nusselt numbers distribution for different wall boundary conditions ($Kn_0 = 0.007$ for $T_d = 20^{\circ}K$ and $Kn_0 = 0.019$ for $T_d = 500^{\circ}K$).

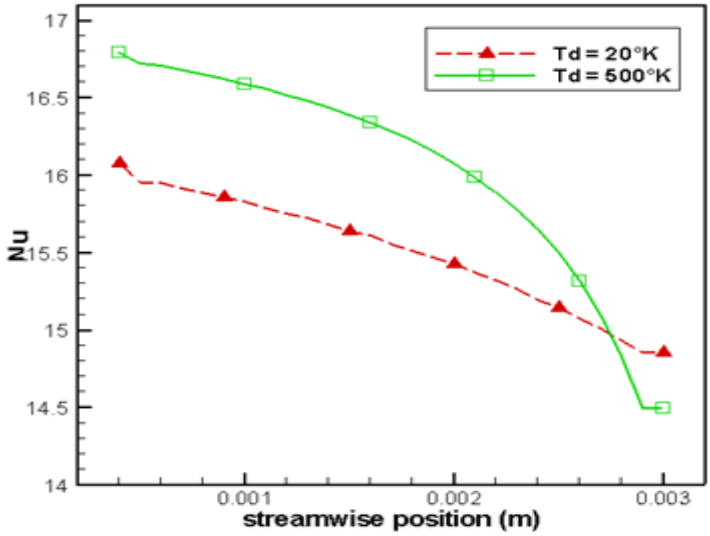

Figure-8. Nusselt numbers distribution for different wall boundary conditions ($Kn_0 = 0.007$).

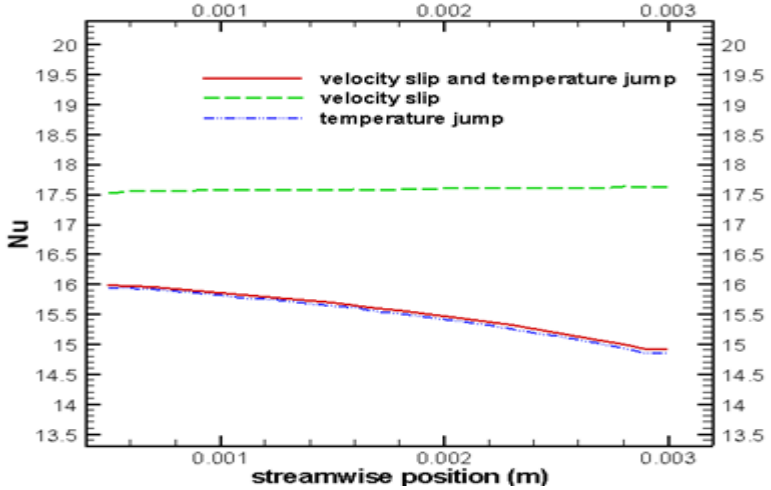

The effects of temperature difference on different boundary conditions are investigated and the results are depicted through Figure 9. The dash-dotted line shows the Nusselt numbers distribution for temperature difference $500^{\circ}K$ and the solid line shows the Nusselt numbers distribution for temperature difference $20^{\circ}K$. In all the three cases the maximum outlet Knudsen number varies up to 0.019 and the Nusselt number for temperature difference $500^{\circ}K$ is higher than that of temperature difference $20^{\circ}K$. The result shows that if only the velocity slip boundary condition is applied on the walls, the temperature difference has no significant effect on the Nusselt numbers and shows a negligible increment along the streamwise direction.

Figure-9. Effect of temperature difference on Nusselt numbers (Kn_0 = 0.007 for T_d = 20°K and Kn_0 = 0.019 for T_d = 500°K).

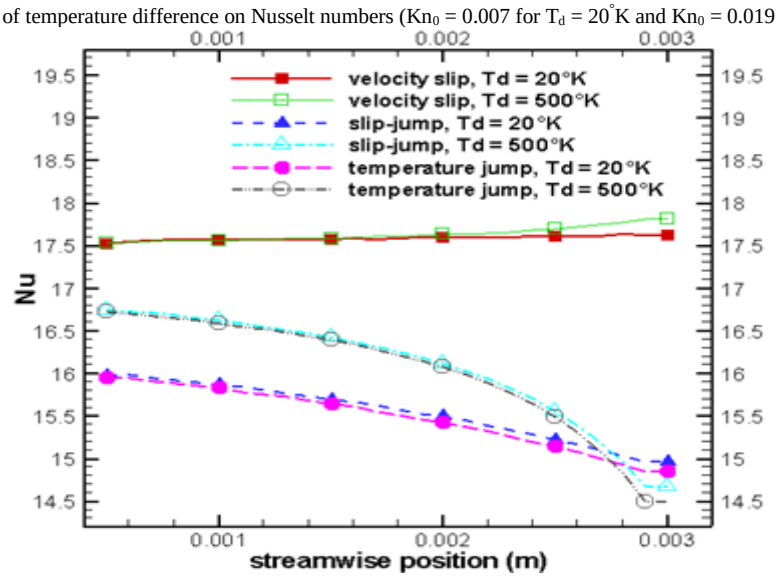

On the other hand if only the temperature jump or both the velocity slip and temperature jump boundary conditions are applied on the walls, the temperature difference shows significant effect on Nusselt numbers.

Figure-10. Nusselt numbers distribution with respect to Knudsen numbers for velocity slip boundary condition (T_d = 500°K).

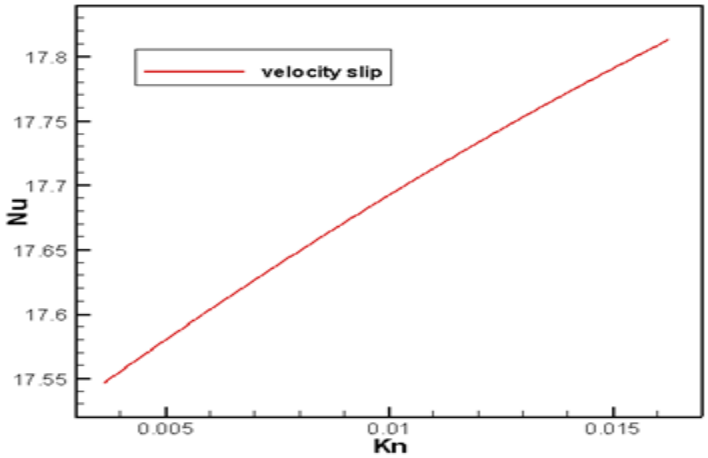

For both the cases the Nusselt numbers decrease along the streamwise position. The Nusselt numbers in the former case is negligible with compared to the later cases.

The Figs. 10 – 12 show the Nusselt numbers distribution against Knudsen numbers for the boundary conditions velocity slip, temperature jump and the combined velocity slip and temperature boundary conditions respectively for the temperature difference 500°*K*.

Figure-11. Nusselt numbers distribution with respect to Knudsen numbers for temperature jump boundary condition (T_d = 500°K).

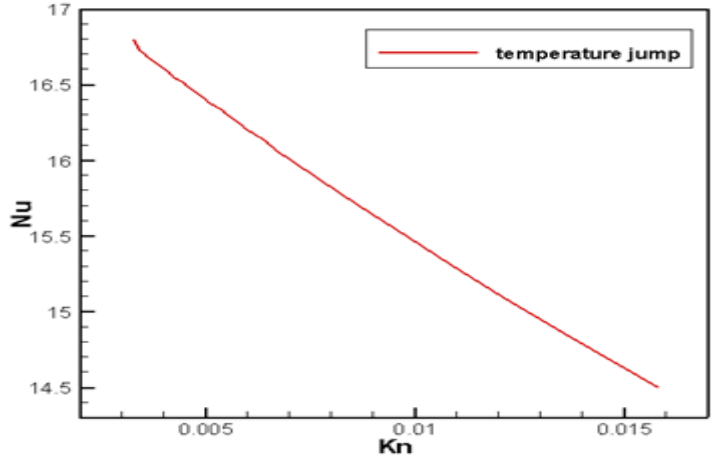

The Figure 10 shows that the Nusselt number increases from 17.53 at position *L/6* to 17.78 at position *9L/10* for the corresponding increase of Knudsen number from 0.003 to 0.014 for the slip velocity boundary condition.

Figure-12. Nusselt numbers distribution with respect to Knudsen numbers for combined velocity slip and temperature jump boundary conditions ($T_d = 500^{\circ}K$).

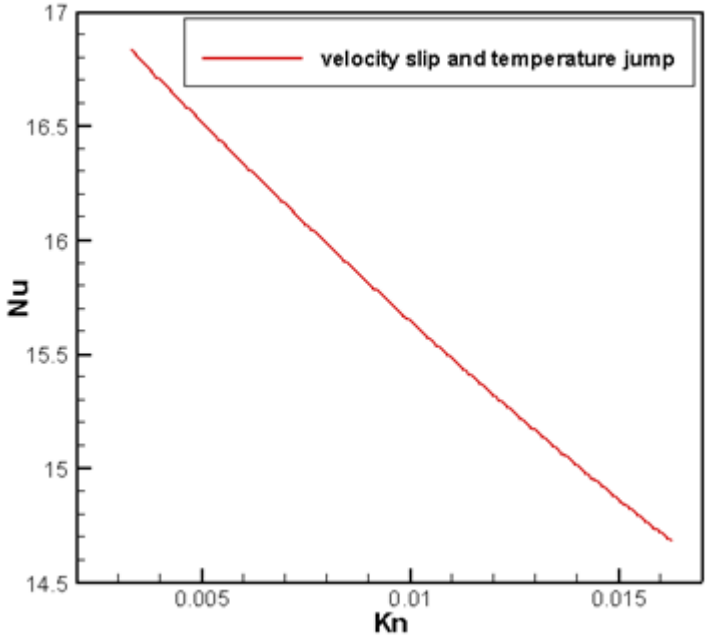

The Fig. 11 shows that the Nusselt number decreases from 16.72 at position *L/6* to 14.83 at position *9L/10* for the corresponding increase of Knudsen number from 0.003 to 0.014 for the temperature jump boundary condition.

The Fig. 12 shows that the Nusselt number decreases from 16.75 at position *L/6* to 14.95 at position *9L/10* for the corresponding increase of Knudsen number from 0.003 to 0.014 for the velocity slip and temperature jump boundary conditions.

3. Conclusions

For asymmetric wall thermal condition when viscous heating is not considered, heat transfer is susceptible to both the Reynolds number and temperature difference. At constant temperature difference, Nusselt number is higher for higher Reynolds number. At fixed Reynolds number the Nusselt number is lower for higher temperature difference.

For symmetric wall thermal condition temperature difference has significant effect on Nusselt number. The Nusselt number is higher for higher temperature difference than that of lower temperature difference for only temperature jump or both velocity slip and temperature jump boundary conditions to the downward direction. But for velocity slip boundary condition the temperature difference has small effect on Nusselt numbers.

For velocity slip boundary condition, Nusselt number increases with the increase of Knudsen number where as for temperature jump boundary condition or both boundary conditions of velocity slip and temperature jump, the Nusselt number decreases with the increase of Knudsen numbers.

References

[1] Gad-el-Hak, M., 2006. *The MEMS handbook*. 2nd ed. New York Taylor and Francis: CRC press.

[2] Schaaf, S. and Chamber, P., 1961. *Flow of rarefied gases*. Princeton University Press: Princeton.

[3] Tuckerman, D. B. and Pease, R. F. W., 1981. "High-performance heat sinking for vlsi." *IEEE Electron Device Letters*, vol. 2, pp. 126-129.

[4] Peiyi, W. and Little, W. A., 1984. "Measurement of the heat transfer characteristics of gas flow in fine channel heat exchangers used for microminiature refrigerators." *Cryogenics*, vol. 24, pp. 415–420.

[5] Peng, X. F. and Peterson, G. P., 1995. "The effect of thermofluid and geometrical parameter on convection of liquids through rectangular microchannels." *Int. J. Heat Mass Transfer*, vol. 38, pp. 755-758.

[6] Peng, X. F., Peterson, G. P., and Wang, B. X., 1994. "Heat transfer characteristics of water flowing through microchannels." *Exp. Heat Transfer*, vol. 7, pp. 265–283.

[7] Nicolas, G., Hadjiconstantinou, and Olga, S., 2002. "Constant-wall-temperature nusselt number in micro and nano-channels." *Journal of heat Transfer*, vol. 124, pp. 356-364.

[8] Wu, H. Y. and Cheng, P., 2003. "An experimental study of convective heat transfer in silicon microchannels with different surface conditions." *Int. J. Heat Mass Transfer*, vol. 46, pp. 2547-2556.

[9] Owhaib, W. and Palm, B., 2004. "Experimental investigation of single phase convective heat transfer in circular microchannels." *Experimental Thermal and Fluid Science*, vol. 28, pp. 105–110.

[10] Chien-Hsin, C., 2006. "Slip-flow heat transfer in a microchannel with viscous dissipation." *Heat Mass Transfer*, vol. 42, pp. 853-860.

[11] Patric, H. O. and William, E. C., 1997. *Compressible fluid flow*. New York: Mc_GrawHill Companies.

[12] Maxwell, J. C., 1879. "On stresses in rarified gases arising from inequalities of temperature." *Philos. Trans. R. Soc.*, vol. 170, pp. 231-256.

[13] Smoluchowski, M., 1898. "Über den Temperatursprung bei Wärmeleitung in Gasen Akad. Wiss. Wien. C." vol. VII, pp. 304-329.
[14] Ansys Inc, 2013. *Ansys fluent theory guide (release 15.0)*. Canonsburg.
[15] Orhan, A. and Mete, A., 2007. "Analysis of laminar heat transfer in micro-poiseuille flow." *International Journal of Thermal Sciences,* vol. 46, pp. 30-37.